On the self-averaging of dispersion for transport in quasi-periodic random media

2007 J. Phys. A: Math. Theor. 40 597

(http://iopscience.iop.org/1751-8121/40/4/002)

INSTITUTE OF PHYSICS PUBLISHING JOURNAL OF PHYSICS A: MATHEMATICAL AND THEORETICAL

J. Phys. A: Math. Theor. **40** (2007) 597–610 doi:10.1088/1751-8113/40/4/002

On the self-averaging of dispersion for transport in quasi-periodic random media

J P Eberhard[1], **N Suciu**[2] **and C Vamoş**[3]

[1] Simulation in Technology, University of Heidelberg, Im Neuenheimer Feld 368, D-69120 Heidelberg, Germany
[2] Institute of Applied Mathematics, University of Erlangen-Nuremberg, Martensstr. 3, D-91058 Erlangen, Germany
[3] 'Tiberiu Popoviciu' Institute of Numerical Analysis, Cluj Napoca branch of the Romanian Academy, PO Box 68-1, 400320, Cluj Napoca, Romania

E-mail: eberhard@uni-hd.de

Received 2 June 2006, in final form 5 November 2006
Published 9 January 2007
Online at stacks.iop.org/JPhysA/40/597

Abstract

In this study we present a numerical analysis for the self-averaging of the longitudinal dispersion coefficient for transport in heterogeneous media. This is done by investigating the mean-square sample-to-sample fluctuations of the dispersion for finite times and finite numbers of modes for a random field using analytical arguments as well as numerical simulations. We consider transport of point-like injections in a quasi-periodic random field with a Gaussian correlation function. In particular, we focus on the asymptotic and pre-asymptotic behaviour of the fluctuations with the aid of a probability density function for the dispersion, and we verify the logarithmic growth of the sample-to-sample fluctuations as earlier reported in Eberhard (2004 *J. Phys. A: Math. Gen.* **37** 2549–71). We also comment on the choice of the relevant parameters to generate quasi-periodic realizations with respect to the self-averaging of transport in statistically homogeneous Gaussian velocity fields.

PACS numbers: 05.10.Gg, 47.55.Mh

1. Introduction

The temporal behaviour of dispersion for transport in heterogeneous media has been considered in the literature for a long time. In this context the stochastic approach has proven successful for predicting the behaviour of transport parameters, see [2–4, 9, 13, 21]. The stochastic approach proposes a generic description of contaminant transport in real systems via averages over the flow realizations [2, 3]. It assumes that the heterogeneity of the flow can be efficiently described through random space functions. Hence, representative transport parameters are

derived from appropriately defined averages over the ensemble of the random flow realizations. An up-scaling of this generic process to a Gaussian process with constant coefficients, called 'macrodispersion', is heuristically inferred from arguments based on the central limit theorem, see [2]. A proof for the existence of the up-scaled process in the case of purely advective transport with a non-vanishing mean velocity was done under the assumption that the random velocity has small fluctuations and suitable strong-mixing properties [13]. However, this proof can be extended to advection–diffusion processes only provided that the diffusion coefficient is of the order of the velocity variance, see [21]. It is worth to note that such an up-scaling can only be proven for ensemble averaged concentrations and does not ensure that single representatives of the ensemble have the same up-scaling, see [18]. The predictive value of the 'macrodispersion concept' for actual realizations is still an open issue and recent studies about this topic are in slight disagreement [12, 19]. The study to what extent the dispersion coefficients represent the behaviour in a single realization is therefore of significant importance. The self-averaging property of the dispersion coefficients renders the macrodispersion coefficients being representative for actual transport realizations [1], provided that a macrodispersive up-scaling of the mean concentration exists [18]. An important advance has been recently reported in [7] where the sample-to-sample fluctuations of the effective transport parameters are analysed by a novel approximation technique. It is shown in [7] that the self-averaging behaviour can be expected for transport in Gaussian velocity fields with finite correlation scales and small variances. This result has been reinforced by numerical simulations of the un-approximated transport problem. The latter further indicates an 'ergodic' behaviour, in the sense that space-averaged coarse-grained concentrations in actual realizations tend to the up-scaled macrodispersion solution in the mean-square limit [18].

In the present work, we continue the analysis of Eberhard [7] using analytical methods for the probability density function of the dispersion coefficient as well as numerical simulations with the Langevin iteration method (LIM). The numerical results given by LIM have recently shown to agree with direct numerical simulations done with a global random walk method [17]. The novelty of the LIM approach consists in providing an explicit expression of dispersion coefficients in given realizations of the random velocity field, approximated for small velocity fluctuations. This approach is feasible whenever single-velocity realizations are available in analytical form, as for instance in the case of quasi-periodic random fields. As Gaussian fields can be approximated by quasi-periodic fields with large numbers of harmonics, it has been shown, based on LIM computations, that for a Gaussian random field the asymptotic value of the longitudinal dispersion coefficient is self-averaging [7]. Moreover, the approach of Eberhard [7] also provides for the first time a numerical evidence that transport in quasi-periodic fields with finite numbers of modes is not self-averaging. In this paper, we study the self-averaging of the dispersion by the mean-square sample-to-sample fluctuations for finite times and finite numbers of modes of the quasi-periodic fields. In particular, we focus on the asymptotic and pre-asymptotic behaviour of the fluctuations with the aid of the probability density function for the dispersion coefficient. We are able to verify the logarithmic growth as previously reported in [7]. We also annotate the selection of the relevant parameters to generate quasi-periodic realizations with respect to the self-averaging. These parameters are the number of modes N_p and the number of realizations R for the ensemble average. And we show that quasi-periodic fields can be used to simulate a self-averaging behaviour of transport in Gaussian velocity fields.

We carry out the LIM investigation on self-averaging for a typical problem of transport in saturated aquifers where the porosity is assumed to be constant even though it may vary weakly. The approach is based on a first-order approximation of the Darcy velocity through quasi-periodic random fields, which has the advantage to yield explicit expressions for the

effective coefficients in single realizations of the transport. This approximation, in the form of the Kraichnan routine, was already successfully used in numerical investigations on large scale behaviour of the effective coefficients in the past, see [5–7, 11, 16, 18]. We consider a velocity field $\mathbf{V}$ with a constant mean $\mathbf{U} = \langle \mathbf{V} \rangle$, where $\langle \cdot \rangle$ denotes the ensemble average over the random flow realizations. The velocity fluctuations $u_i = V_i - U_i, i = 1, 2, 3$, are computed as a superposition of N_p cosine modes,

$$u_i(\mathbf{x}) = |\mathbf{U}| \sqrt{\frac{2q_0}{N_p}} \sum_{l=1}^{N_p} p_i(\mathbf{q}_l) \cos(\mathbf{q}_l \cdot \mathbf{x} + \alpha_l), \tag{1}$$

where the wave vectors $\mathbf{q}_l$ are independent normal distributed random variables with zero mean and variance l_0^{-2}. The phases α_l are uniformly distributed in the interval $[0, 2\pi]$, and the functions $p_i(\mathbf{q}) = \delta_{1i} - q_1 q_i / \mathbf{q}^2, i = 1, 2, 3$, are projectors which ensure the incompressibility of the flow. For $N_p \to \infty$, (1) tends to a Gaussian velocity field with the zero mean and isotropic Gaussian shaped correlation function $\sim \exp\left(-\mathbf{x}^2 / l_0^2\right)$, which approximates the Darcy flow for log-hydraulic conductivity with a variance q_0 and an isotropic Gaussian correlation with a correlation length l_0, see e.g. [7].

2. Transport and dispersion in random media

We consider the transport of solutes in two- and three-space dimensions by advection–diffusion processes. The trajectory $X_i(t), i = 1, 2, 3$, of a solute molecule depends on three factors: the isotropic local dispersion with constant coefficient D_0, described as a Wiener process $\mathbf{W}$; the large scale variability of the velocity field, described by a statistically homogeneous random field $\mathbf{V} = \mathbf{U} + \mathbf{u}$; and the initial position $\mathbf{X}_0$. In the following we consider only point-like injections, and without loss of generality, we assume $\mathbf{U} = U\mathbf{e}_1$ and $\mathbf{X}_0 = 0$.

For a given realization of the velocity field, the transport is described by the integral form of the Langevin equation:

$$X_i(t) = U\delta_{i1}t + \int_0^t \mathrm{d}t'\, u_i(\mathbf{X}(t')) + \int_0^t \mathrm{d}W_i(t'). \tag{2}$$

The Wiener process $W_i = \int_0^t \mathrm{d}W_i(t')$ has the properties $\langle W \rangle_{\mathbf{w}} = 0$ and $\langle [W(t)]^2 \rangle_{\mathbf{w}} = 2D_0 t$, where the angular brackets $\langle \cdot \rangle_{\mathbf{w}}$ denote the average over the realizations of the Wiener process. In the case of constant local dispersion coefficient D_0, the integral representation of the solution of the Langevin equation corresponds to the advection–diffusion equation for the normalized concentration, see [8],

$$\partial_t c + \mathbf{V} \cdot \nabla c = D_0 \nabla^2 c.$$

The dispersion of the solute can be conveniently described by the variance of the displacements of the solute molecules, i.e. the second-order central moment of the actual concentration in a given realization of the velocity field. The diagonal components of the second moment tensor are given by

$$S_{ii}(t) = \langle [x_i(t) - \langle x_i(t) \rangle_{\mathbf{w}}]^2 \rangle_{\mathbf{w}}. \tag{3}$$

Since we analyse only the longitudinal dispersion in the present study, we drop the subscripts hereafter. The dispersion can easily be described by a dispersion coefficient defined by half of the rate of the increase of the second moment, i.e., $S(t)/(2t)$. For $t \to 0$, $S(t)$ yields the local variance around the initial condition, and the dispersion coefficient above defines the local dispersion coefficient D_0 in (2) (see e.g. [8]). It also defines an effective diffusion coefficient if its limit is finite for $t \to \infty$ [17].

The most common definition of the dispersion coefficient is given by the time derivative of the second moment $S(t)$,

$$D(t) = \frac{1}{2}\frac{\mathrm{d}S(t)}{\mathrm{d}t}. \tag{4}$$

Definition (4) for the dispersion coefficient is preferred in analytical approaches [5–7] because it reduces the number of time quadratures in the resulting quantity. However, at finite times, when $D(t)$ does not play the role of a diffusion coefficient in a local equation of transport [17], the dispersion coefficients can be used merely as equivalent representations of the actual dispersion described by the moments (3). Obviously, when the effective coefficients can be defined in the large time limit, $D(t) = (1/2)\mathrm{d}S/\mathrm{d}t$ coincides with its time average $S/(2t)$. We refer to [17] for a more detailed discussion of the two definitions of dispersion.

In the stochastic approach for the transport problem, the mean value of the dispersion coefficient (4) is estimated by the average over the ensemble of the velocity realizations, i.e., $\langle D(t)\rangle$. The mean-square sample-to-sample fluctuations $\delta D(t)$ of the coefficients $D(t)$ are defined by

$$(\delta D(t))^2 = \langle (D(t))^2\rangle - \langle D(t)\rangle^2. \tag{5}$$

The same definitions will be used throughout the paper for the mean and fluctuations of the time average $S/(2t)$ of the coefficient D.

2.1. Approximation method

The Langevin iteration approximation for (2) consists of the first iteration of the Langevin equation about the 'unperturbated' problem for dispersion in the mean flow **U**, see [7]:

$$X_i(t) = U\delta_{i1}t + \int_0^t \mathrm{d}t'\, u_i\left[U\delta_{i1}t' + \int_0^{t'} \mathrm{d}W_i(t'')\right] + \int_0^t \mathrm{d}W_i(t'). \tag{6}$$

Numerical arguments indicate that (6) yields asymptotic approximations in the velocity fluctuations which are equivalent to those of a large class of iterative methods [17]. The evaluation and direct comparison with accurate numerical simulations, also done in [17], show that the LIM based on (6) yields very good approximations at times larger than the dispersion time scale l_0^2/D_0. Hence the numerical computation of these expressions, followed by the ensemble average, allows us to evaluate asymptotically the sample-to-sample fluctuations of the effective coefficients.

For the numerical computations in sections 3 and 4, we consider therefore the explicit LIM analytical expressions for $D(t)$ in single realizations of the transport given in appendix B.1 of [7]. Using equations (1), the latter can easily be computed numerically for the two- and three-dimensional case (as done in [17, 7]).

2.2. Asymptotic dispersion coefficient

We also consider the fluctuations of the longitudinal dispersion coefficient for $t \to \infty$. The result given by the Langevin iteration method and the perturbation theory approach for $D\,(t \to \infty)$ (see equation (16) in [7]) yields

$$D^\infty = D_0 + \frac{q_0 U^2}{N_p}\sum_j{}^{*}\, p_1(\mathbf{q}^{(j)})^2 \frac{1/\tau_D^{(j)}}{\left(1/\tau_D^{(j)}\right)^2 + \left(1/\tau_u^{(j)}\right)^2}, \tag{7}$$

where the wave vectors $\mathbf{q}^{(j)}$ define the realization for N_p cosine modes. The summation is defined by $\sum_j^* := \sum_{j=1}^{N_p}$ for $\mathbf{q}^{(j)} \neq \mathbf{0}$, and the time scales by $\tau_u^{(j)} := 1/\left(Uq_1^{(j)}\right)$ and

$\tau_D^{(j)} := 1/\left(D_0 \mathbf{q}^{(j)^2}\right)$. It is evident that the value of D^∞, equation (7), explicitly depends on the given realization. As the ensemble mean of D^∞ must be independent of the single realizations, the sample-to-sample fluctuations do not vanish for finite numbers of N_p. The ensemble average of the asymptotic dispersion D^∞ is given by (see appendix B.3 in [7])

$$\langle D^\infty \rangle = D_0 + q_0 U l_0 \sqrt{\frac{\pi}{2}} \left(1 - 8\epsilon^4 \exp\left(\frac{1}{2\epsilon^2}\right) \operatorname{erfc}\left(\frac{1}{\sqrt{2}\epsilon}\right) + 8\epsilon^4 - \frac{16\epsilon^3}{\sqrt{2\pi}} + 4\epsilon^2 - \frac{16\epsilon}{3\sqrt{2\pi}}\right),$$

where $\epsilon = \tau_u/\tau_D = D_0/U l_0$. It holds true that $\langle D^\infty \rangle = \lim_{t\to\infty} \langle D(t) \rangle$.

3. Probability density function of D

To analyse the asymptotic behaviour of $(\delta D^\infty)^2$ for $N_p < \infty$ theoretically, we investigate the probability density function of D denoted by $P_D(D)$.

To define the probability density function the dispersion of each realization of the ensemble is considered as a random variable $D(t)$ for fixed times t. With the assumption that the corresponding probability density function $P_D(D)$ is continuous and normalized, the moments are then defined by

$$\langle D^n \rangle = \int_{-\infty}^{\infty} \mathrm{d}D \; P_D(D) D^n, \tag{8}$$

and the probability function is defined according to [20] by

$$P_D(D; t) = \langle \delta(D - D(t)) \rangle, \tag{9}$$

where the average $\langle \cdot \rangle$ is to be taken with respect to the realizations of the quasi-periodic ensemble of aquifer realizations, and $\delta(\cdot)$ denotes Dirac's delta function. To derive $P_D(D)$ the value of $D(t)$ is calculated by the approximation for the dispersion coefficient given by the LIM. However, an explicit result for $P_D(D)$ can be derived only in the long-time regime for three dimensions. In the following we analyse the asymptotic behaviour of $P_D(D)$ in the limit $t \to \infty$. Using the asymptotic dispersion D^∞ given in (7) we obtain

$$P_D(D) \equiv 0 \qquad \text{for} \quad D < D_0, \tag{10}$$

since all emerging corrections to D_0 are positive. For $D \geqslant D_0$, $P_D(D)$ can be rewritten according to (7) and (9) as

$$\begin{aligned} P_D(D) &= \left\langle \delta\left(D - D_0 - \frac{q_0 U^2}{N_p} \sum_j{}^{*} p_1(\mathbf{q}^{(j)})^2 \frac{1/\tau_D^{(j)}}{\left(1/\tau_D^{(j)}\right)^2 + \left(1/\tau_u^{(j)}\right)^2}\right)\right\rangle \\ &= \int \mathrm{d}^3 q^{(1)} P_{\mathbf{q}}(\mathbf{q}^{(1)}) \cdots \int \mathrm{d}^3 q^{(N)} P_{\mathbf{q}}(\mathbf{q}^{(N)}) \\ &\quad \times \delta\left(D - D_0 - \frac{q_0 U^2}{N_p} \sum_j{}^{*} p_1(\mathbf{q}^{(j)})^2 \frac{D_0 \mathbf{q}^{(j)^2}}{\left(D_0 \mathbf{q}^{(j)^2}\right)^2 + \left(U q_1^{(j)}\right)^2}\right), \end{aligned} \tag{11}$$

where $P_{\mathbf{q}}(\mathbf{q})$ is given by $P_{\mathbf{q}}(\mathbf{q}) = (2\pi)^{-d/2} l_0^d \exp\left(-\mathbf{q}^2 l_0^2/2\right)$. As shown in appendix A we obtain for the asymptotic result of $P_D(D)$ for D^∞

$$P_D(D) \sim \frac{q_0^2 U^2 l_0^2}{\epsilon \sqrt{2\pi} N_p^2} D^{-3}, \tag{12}$$

which is of the order $O\left(q_0^2\right)$. Due to the definition of the second moment $\langle D^2 \rangle$, see (8), the result for $P_D(D)$ implies $P_D(D) D^2 \sim D^{-1}$. It follows that the integral $\langle (D^\infty)^2 \rangle =$

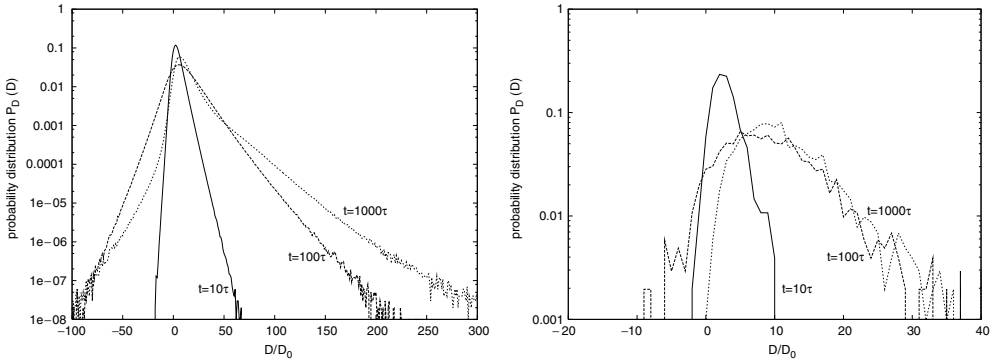

Figure 1. Probability density function $P_D(D)$ for $D = (1/2)\mathrm{d}S/\mathrm{d}t$ from the result of the LIM (left) and for $S/(2t)$ (right). The function is computed by 10^8 realizations (left) and 1024 realizations (right), respectively, for $N_p = 64$, $q_0 = 0.1$, and $\epsilon = 0.01$, for different times t. The ensemble means are given by $\langle D\rangle/D_0 = 4.2$ and $\langle S/(2t)\rangle/D_0 = 2.6$ for $t = 10\tau$, $\langle D\rangle/D_0 = 10.8$ and $\langle S/(2t)\rangle/D_0 = 8.2$ for $t = 100\tau$, and $\langle D\rangle/D_0 = 13.0$ and $\langle S/(2t)\rangle/D_0 = 11.9$ for $t = 1000\tau$.

$\int \mathrm{d}D\ P_D(D)D^2 \sim \int \mathrm{d}D\ D^{-1}$, that is the second moment, yields a logarithmic dependence of the fluctuations on D, i.e., the fluctuations behave as $\sim \ln(D)$. In contrast, the ensemble average $\langle D^\infty\rangle$ exists for $P_D(D) \sim D^{-3}$. Hence, the results show that in the given approximation the asymptotic sample-to-sample fluctuations $(\delta D^\infty)^2 = \langle (D^\infty)^2\rangle - \langle D^\infty\rangle^2$ do not exist. The asymptotic behaviour given by $P_D(D)D^2 \sim D^{-1}$ for the integral of $\langle (D^\infty)^2\rangle$ implies a logarithmic growth of the fluctuations which agrees with the results of [7].

3.1. Numerical computation of $P_D(D)$

Next we compute $P_D(D)$ numerically by calculating the dispersion coefficient $D(t)$ for up to 10^8 realizations of the random quasi-periodic field for three dimensions. In addition to $P_D(D)$ for the asymptotic dispersion (12), $P_D(D)$ is also computed numerically for finite times t. The numerical results for the asymptotic temporal behaviour of the probability density function for $D = D^\infty$ are shown in appendix B.

The longitudinal dispersion is given by the result of the Langevin iteration method. This means that we compute $D(t)$ for a set of fixed time points using the explicit results given by the LIM [7], see section 2.1. $P_D(D)$ is numerically calculated as a discrete probability density function using dispersion bins of length 10^{-2}. Each bin adds up the number of values D falling into the corresponding bin. Hence, $P_D(D)$ is the counted number of each bin divided by the number of realizations. The discrete functions are computed for fields with variance $q_0 = 0.1$, $U = 1\mathrm{m/day}$, correlation length $l_0 = 1\mathrm{m}$, and local diffusion $D_0 = 0.01\,\mathrm{m}^2/\mathrm{day}$ for different times t and numbers N_p. Hereafter the symbol m defines meters and $\tau = l_0/U$ the advective time scale.

Figures 1–3 depict the probability functions for times $t = 10\tau$, $t = 100\tau$, and $t = 1000\tau$. The number of modes is fixed to $N_p = 64, 640$ and $N_p = 6400$, respectively. On the left-hand side of figures 1–3, $P_D(D)$ is calculated for the dispersion coefficient $D(t) = (1/2)\,\mathrm{d}S/\mathrm{d}t$, and on the right-hand side for $S/(2t)$.

As a result of the numerical computation on $P_D(D)$ shown in figures 1 and 2, it follows that the larger the time the higher the probability for the large values of $D \gg \langle D\rangle$. Fitting the tail of the numerical results for $D(t) = (1/2)\,\mathrm{d}S(t)/\mathrm{d}t$ to a function proportional to $D^{-\alpha}$ using a nonlinear least-squares Marquardt–Levenberg algorithm [15] yields for $N_p = 64$

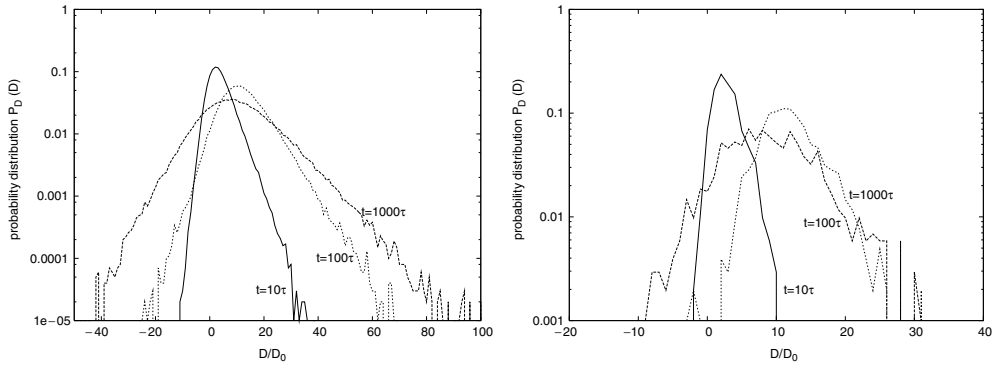

Figure 2. Probability density function $P_D(D)$ for $D = (1/2)\mathrm{d}S/\mathrm{d}t$ from the result of the LIM (left) and for $S/(2t)$ (right). The function is computed by 10^5 realizations (left) and 1024 realizations (right) for $N_p = 640$, $q_0 = 0.1$, and $\epsilon = 0.01$, for different times t. The ensemble means are given by $\langle D\rangle/D_0 = 4.2$ and $\langle S/(2t)\rangle/D_0 = 2.6$ for $t = 10\tau$, $\langle D\rangle/D_0 = 10.7$ and $\langle S/(2t)\rangle/D_0 = 8.1$ for $t = 100\tau$, and $\langle D\rangle/D_0 = 13.0$ and $\langle S/(2t)\rangle/D_0 = 12.0$ for $t = 1000\tau$.

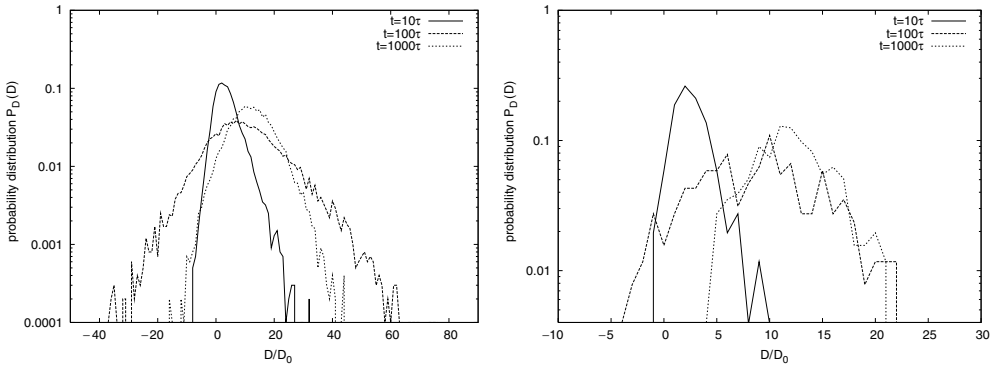

Figure 3. Probability density function $P_D(D)$ for $D = (1/2)\mathrm{d}S/\mathrm{d}t$ from the result of the LIM (left) and for $S/(2t)$ (right). The function is computed by 10^4 realizations (left) and 183 realizations (right) for $N_p = 6400$, $q_0 = 0.1$, and $\epsilon = 0.01$, for different times t. The ensemble means are given by $\langle D\rangle/D_0 = 4.2$ and $\langle S/(2t)\rangle/D_0 = 2.6$ for $t = 10\tau$, $\langle D\rangle/D_0 = 10.6$ and $\langle S/(2t)\rangle/D_0 = 8.2$ for $t = 100\tau$, and $\langle D\rangle/D_0 = 12.9$ and $\langle S/(2t)\rangle/D_0 = 12.0$ for $t = 1000\tau$.

$$\alpha = 3.13 \pm 0.50 \qquad \text{for } t = 10\tau \qquad (D/D_0 \geqslant 15)$$
$$\alpha = 3.01 \pm 0.20 \qquad \text{for } t = 100\tau \qquad (D/D_0 \geqslant 50)$$
$$\alpha = 3.00 \pm 0.13 \qquad \text{for } t = 1000\tau \qquad (D/D_0 \geqslant 205),$$

for $N_p = 640$

$$\alpha = 3.01 \pm 0.20 \qquad \text{for } t = 10\tau \qquad (D/D_0 \geqslant 7)$$
$$\alpha = 3.05 \pm 0.16 \qquad \text{for } t = 100\tau \qquad (D/D_0 \geqslant 31)$$
$$\alpha = 2.86 \pm 0.16 \qquad \text{for } t = 1000\tau \qquad (D/D_0 \geqslant 13),$$

and for $N_p = 6400$

$$\alpha = 3.12 \pm 0.66 \qquad \text{for } t = 10\tau \qquad (D/D_0 \geqslant 8)$$
$$\alpha = 3.02 \pm 0.47 \qquad \text{for } t = 100\tau \qquad (D/D_0 \geqslant 26)$$
$$\alpha = 2.89 \pm 0.26 \qquad \text{for } t = 1000\tau \qquad (D/D_0 \geqslant 11).$$

These numerical results fully agree with the analytical result (12). Further it is evident that the probability density functions P_D as a function of time t increase with growing time for the large values of D, that is, the fluctuations of $D(t)$ around the mean increase with growing time. This result fully agrees with the fact that the sample-to-sample fluctuations do not converge for $t \to \infty$. For finite times, however, the fluctuations around the mean are finite and the sample-to-sample fluctuations $\langle (D(t) - \langle D(t) \rangle)^2 \rangle$ cannot be divergent.

In addition, we would like to round off the numerical computation of $P_D(D)$ by noting the values for the asymptotic behaviour of the probability density function computed for the dispersion coefficient $S/(2t)$. Due to the small number of realizations for the computation of $P_D(D)$ using $D = S/(2t)$ the numerical results for the asymptotic behaviour of the probability density functions show large deviations (see right plots in figures 1–3). Fitting the tail of the numerical results to a function proportional to $D^{-\alpha}$ for $D = S/(2t)$ yields for $N_p = 64$

$$\begin{aligned} &\alpha = 4.01 \pm 0.41 \qquad \text{for } t = 10\tau \qquad (D/D_0 \geqslant 6) \\ &\alpha = 3.09 \pm 0.23 \qquad \text{for } t = 100\tau \qquad (D/D_0 \geqslant 15) \\ &\alpha = 2.75 \pm 0.20 \qquad \text{for } t = 1000\tau \qquad (D/D_0 \geqslant 13), \end{aligned}$$

for $N_p = 640$

$$\begin{aligned} &\alpha = 4.03 \pm 0.61 \qquad \text{for } t = 10\tau \qquad (D/D_0 \geqslant 7) \\ &\alpha = 4.14 \pm 0.30 \qquad \text{for } t = 100\tau \qquad (D/D_0 \geqslant 15) \\ &\alpha = 4.34 \pm 1.63 \qquad \text{for } t = 1000\tau \qquad (D/D_0 \geqslant 21), \end{aligned}$$

and for $N_p = 6400$

$$\begin{aligned} &\alpha = 3.71 \pm 0.72 \qquad \text{for } t = 10\tau \qquad (D/D_0 \geqslant 4) \\ &\alpha = 3.38 \pm 0.48 \qquad \text{for } t = 100\tau \qquad (D/D_0 \geqslant 15) \\ &\alpha = 3.87 \pm 0.49 \qquad \text{for } t = 1000\tau \qquad (D/D_0 \geqslant 10). \end{aligned}$$

4. Numerical results for the temporal behaviour of the mean and sample-to-sample fluctuations

We investigate the self-averaging of the longitudinal dispersion coefficient. The latter is addressed by computing the temporal sample-to-sample fluctuations. The Langevin iteration method yields an explicit result for the longitudinal coefficient $D(t)$ defined by (4), see equation (B1) in [7]. The ensemble mean is then computed by numerical averaging over the explicit result for the different numbers of realizations R and different numbers of modes N_p, and the sample-to-sample fluctuations of the dispersion coefficients D are computed by (5).

For the numerical computations we consider divergence-free velocity fields given by Darcy's law for normal log-hydraulic conductivity in two and three dimensions. The fields are Gaussian correlated using the parameters as given in section 3.1, and in each realization we consider an isotropic local diffusion $D_0 = 0.01\text{m}^2/\text{day}$. The fields are numerically generated (in first-order approximation in $q_0^{1/2}$) with the aid of (1) as done in [5–7, 11, 16]. To assess the reliability of the procedure, the simulations are repeated for increasing numbers N_p of modes used in the Kraichnan routine ($N_p = 64$, 640, and $N_p = 6400$). In [18], it is shown that the so generated velocity fields fulfill the requirements of the limit theorem given in [13]. The numerical computation of the longitudinal dispersion coefficient, equation (B1) in [7], is conducted for dimensionless times $t/\tau = Ut/l_0$ corresponding to 3900 correlation lengths. Ensembles of up to 1024 realizations of the transport simulations are computed for each of the three N_p values.

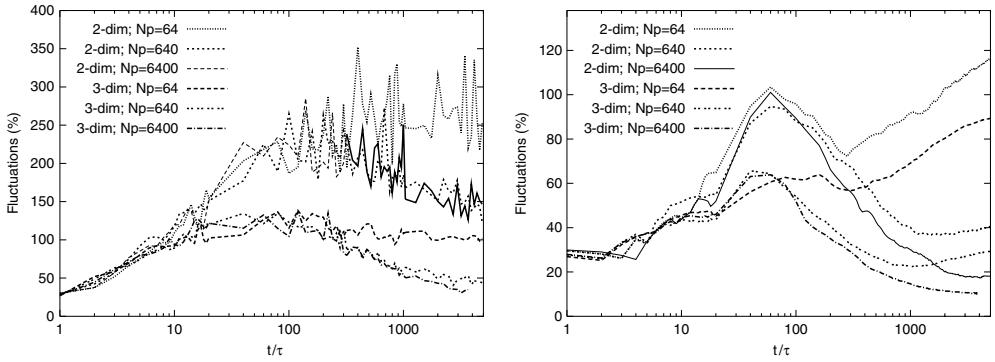

Figure 4. The relative sample-to-sample fluctuations of the longitudinal dispersion coefficients computed by the Langevin iteration method for fixed $R = 256$, and $N_p = 64$, 640 and $N_p = 6400$. The dispersion coefficients are computed by $(1/2)\,\mathrm{d}S(t)/\mathrm{d}t$ (left) and $S(t)/(2t)$ (right), respectively. For the three-dimensional case and $N_p = 6400$, the number of realizations is $R = 183$.

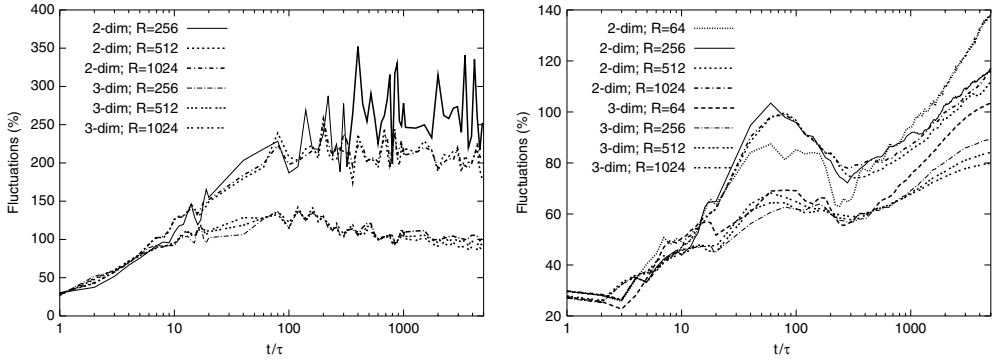

Figure 5. The relative sample-to-sample fluctuations of the longitudinal dispersion coefficients for increasing R and fixed $N_p = 64$. $D(t)$ is computed by $(1/2)\,\mathrm{d}S(t)/\mathrm{d}t$ for the left plot and by $S(t)/(2t)$ for the right plot.

4.1. Self-averaging behaviour of the effective coefficients

In figures 4 and 5, the relative sample-to-sample fluctuations $\delta D(t)/\langle D(t)\rangle$ are computed and compared for the different values of N_p and R. Figure 4 shows the sample-to-sample fluctuations of the longitudinal dispersion coefficients computed by the Langevin iteration method for fixed $R = 256$, and increasing N_p. The dispersion coefficients are computed by $D(t) = (1/2)\,\mathrm{d}S/\mathrm{d}t$ (left plot in figure 4) and $S(t)/(2t)$ (right plot in figure 4), respectively. The plots show the dependence of the fluctuations on N_p for two- and three-space dimensions. Figure 5 depicts the sample-to-sample fluctuations of the longitudinal dispersion coefficients for increasing the number of realizations R and fixed $N_p = 64$. D is computed by $D(t)$, (4), for the left plot, and by $S(t)/(2t)$ for the right plot. As shown in the plots of figure 5, the increase of R over hundreds of realizations does not enhance the self-averaging behaviour of D and $S/(2t)$.

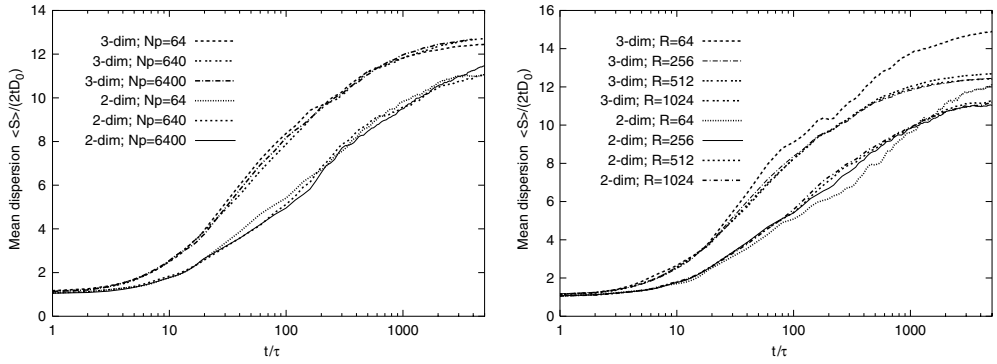

Figure 6. The mean longitudinal dispersion for fixed $R = 256$ and $N_p = 64$, 640 and $N_p = 6400$ (left), and for $N_p = 64$ fixed and increasing R (right). The graphs show the dependence on N_p and R, respectively, for two- and three-spatial dimensions. For the three-dimensional case and $N_p = 6400$, the number of realizations is fixed to $R = 183$.

For $N_p = 64$ and $N_p = 640$, the numerical results of the LIM exhibit a slow increase of the fluctuations at large times for two and three spatial dimensions, as shown in figure 4 (right). However, for $N_p = 6400$, the fluctuations (for both the two- and three-dimensional cases) drop below 20% at about 4000 advection time scales τ, see figure 4. This behaviour indicates that the longitudinal dispersion coefficient for transport in Gaussian fields, approximated by (1) using large numbers of modes N_p, tends to the ensemble average in the mean-square limit for $t \to \infty$. The numerical results in figure 4 also show that the larger the simulation time the larger the N_p to capture the self-averaging property, i.e., the sample-to-sample fluctuations decrease with growing simulation time. Further, it is obvious from figure 4 (right) that transport in three dimensions exhibits better self-averaging properties than in two-spatial dimensions. We would like to remark that the dispersion coefficient $D(t)$ is more noisy than the time average $S(t)/(2t)$. This can clearly be seen by the different percentage scale of the fluctuations in the plots of figures 4 and 5 (see also [17]).

For the mean longitudinal coefficient $\langle D(t)\rangle$, however, the plots in figure 6 show that a few hundred realizations are sufficient for a good result of the ensemble coefficient. Figure 6 displays the mean longitudinal dispersion $\langle S\rangle$, normalized by the local dispersion $2tD_0$, for fixed $R = 256$ and increasing N_p on the left, and for $N_p = 64$ and increasing R on the right. The graphs therefore display the dependence of the mean dispersion coefficient $\langle S(t)/(2t)\rangle$ on N_p and R, respectively, for two and three dimensions. These numerical results indicate that the means are very robust against variations in the number of modes N_p of the underlying random field. The results also show that the difference in the transport behaviour is significant for two- and three-space dimensions.

The results presented in figure 6 indicate that the use of the Kraichnan routine is reasonable for simulating diffusive transport in groundwater flow governed by Darcy's law. The routine ensures the evolution of the ensemble averaged process towards the up-scaled macrodispersion process. Further, figures 4 and 5 bring a numerical evidence for the self-averaging behaviour of transport in the Darcy flows when the latter are approximated by quasi-periodic random fields generated with the Kraichnan routine for $N_p = 6400$ and hundreds of realizations.

As a result, the representation (1) of the groundwater flow through quasi-periodic random fields approximates the self-averaging behaviour of the effective coefficients if the number of periods is large enough ($N_p = 6400$ for a simulation time of 1000τ). The fluctuations'

magnitude does not depend significantly on the number of realizations of the velocity field as shown by figure 5. Figure 4 also indicates that the fluctuations for Gaussian fields are well reproduced when using quasi-periodic fields with N_p of the order of the total simulation time since the fluctuations are the same at time 10τ for $N_p \geqslant 64$, at 100τ for $N_p \geqslant 640$, and at time 1000τ for $N_p \geqslant 6400$. Further, for all N_p values the logarithmic growth begins always after the mentioned times. According to these numerical results we propose for an optimal choice of the relevant parameters the values $N_p \geqslant 6400$ and $R \approx 250$ for about 1000τ.

5. Conclusions

We present a numerical study for the self-averaging of the longitudinal dispersion coefficient for transport in a quasi-periodic random medium. To this end we investigate the sample-to-sample fluctuations of the dispersion for finite times and finite numbers of modes for the random field. We study the probability density function as well as the fluctuations numerically using the Langevin iteration method. Further, we investigate conditions for reliable simulations of the self-averaging behaviour using the Kraichnan routine.

We focus on the pre-asymptotic and asymptotic behaviour of the fluctuations with the aid of the probability density $P_D(D)$. The analytical result for $P_D(D) \sim D^{-3}$ implies that the ensemble average $\langle D^\infty \rangle$ is finite and that the fluctuations $\langle (D^\infty)^2 \rangle - \langle D^\infty \rangle^2$ do not converge. This fact results from the integral $\int D^2 P_D(D) \sim \ln D$, i.e., the fluctuations of the asymptotic dispersion D^∞ increase logarithmically with the dispersion D and independently of time t. This result verifies the logarithmic growth of the sample-to-sample fluctuations as reported in [7]. We show that the numerical result for the asymptotic probability density also agrees with the analytical result and that the probability to get large dispersion values increases with growing time t. So, transport in quasi-periodic velocity fields with a finite number of modes N_p is not self-averaging.

For large numbers of modes N_p the Kraichnan routine (1) approximates the Gaussian random fields where transport is self-averaging, see [7, 13, 18]. Accordingly our numerical simulations of the sample-to-sample fluctuations exhibit the self-averaging behaviour of transport in quasi-periodic random fields for very large numbers of modes ($N_p = 6400$). The simulations also indicate that the fluctuations and the self-averaging behaviour of D do not depend on the number of realizations R of the velocity field. For a given simulation period, the fluctuations are insensitive to the number of realizations R, provided that R is at least a few hundred, but depend strongly on the number of modes N_p. To simulate transport in Gaussian fields we find that N_p needs to be as large as the total simulation time or larger. In particular, for times up to 1000τ a good choice is $N_p \geqslant 6400$ and about $R \approx 250$. So, despite the logarithmic increase of the fluctuations of the dispersion coefficient, quasi-periodic fields can be used to simulate self-averaging behaviour of transport in Gaussian velocity fields for moderate numbers of realizations and large numbers of periodic modes.

One of the prospective areas of application for the presented theory is the characterizing and analysing of porous disordered media. In that field sophisticated ideas of e.g. percolation and fractal geometry have proven useful in explaining the features of the transport properties of single flow for a long time, see e.g. [10, 14]. Self-averaging properties as studied here may potentially round off the characterization of the transport properties of random media (see also e.g. [3, 9]).

Acknowledgments

NS gratefully acknowledges the financial support of Deutsche Forschungsgemeinschaft (DFG grant SU 415/1-1). The work of CV is a contribution to the 'Interdisciplinary Programme for the Prevention of the Major Risk Phenomena at National Level' of the Romanian Academy.

Appendix A. Explicit result for $P_D(D)$

To calculate the probability density function for $D \to \infty$ we start with equation (11) and consider the case $N_p = 1$ first. We obtain for $P_D(D)$, using $P_{\mathbf{q}}(\mathbf{q})$ from section 2.1 of Eberhard [7],

$$P_D(D) = \frac{l_0^3}{\sqrt{2\pi}^3} \int \mathrm{d}^3 q \, \mathrm{e}^{-\frac{1}{2}\mathbf{q}^2 l_0^2} \delta \left(\tilde{D} - c \frac{p_1^2(\mathbf{q})\mathbf{q}^2}{\mathbf{q}^4 + q_1^2 \epsilon^2} \right),$$

where we use $\tilde{D} := D - D_0$ and $c := U^2 q_0 / D_0$. Introducing spherical polar coordinates and scaling the radial variable by $\tilde{D}$, we get

$$P_D(D) = 2 \frac{l_0^2}{\sqrt{2\pi}^3} \frac{1}{\sqrt{\tilde{D}}^5} \int_0^1 \mathrm{d}z \int_0^\infty \mathrm{d}k \, k^2 \, \mathrm{e}^{-\frac{k^2}{2\tilde{D}}} \delta \left(1 - \frac{c(1-z^2)^2}{k^2 + \tilde{D} z^2 \epsilon^2} \right).$$

Performing the integration using Dirac's delta function with restrictions to the integration limits, the probability function yields

$$P_D(D) = \frac{l_0^2}{\sqrt{2\pi}^3} \frac{1}{\sqrt{\tilde{D}}^5} \int_0^{a(\tilde{D})} \mathrm{d}z \sqrt{c(1-z^2)^2 - \tilde{D} z^2 \epsilon^2} \times \exp\left(-\frac{1}{2\tilde{D}} c(1-z^2)^2 + z^2 \epsilon^2 / 2 \right) (1-z^2)^2 c, \tag{A.1}$$

where

$$a(\tilde{D}) = \sqrt{\frac{1}{2c}\left(2c + \epsilon^2 \tilde{D} - \sqrt{4\epsilon^2 \tilde{D} c + \epsilon^4 \tilde{D}^2}\right)}.$$

With the aid of the mean value theorem we obtain for (A.1) passing to the limit $D \to \infty$

$$P_D(D) = \frac{1}{\sqrt{2\pi}} l_0^2 \frac{c^2}{\epsilon} D^{-3} = \frac{U^2 q_0^2 l_0^2}{\epsilon \sqrt{2\pi}} D^{-3}.$$

For a finite number of modes $N_p > 1$ the calculus yields analogous to the case $N_p = 1$ then

$$P_D(D) = \frac{U^2 q_0^2 l_0^2}{\epsilon \sqrt{2\pi} N_p^2} D^{-3}.$$

This result is of the order $O\left(q_0^2\right)$.

Appendix B. Numerical computation of the asymptotic temporal behaviour of $P_D(D)$

We complete the analysis for $P_D(D)$ for $D = D^\infty$ of section 3 showing numerical results for the asymptotic behaviour of the probability density distribution. Therefore, $P_D(D)$ is numerically computed, using (7) for D and dispersion bins of length 10^{-2} as described in section 3.1, for $t \to \infty$ and 10^9 realizations of the random quasi-periodic field.

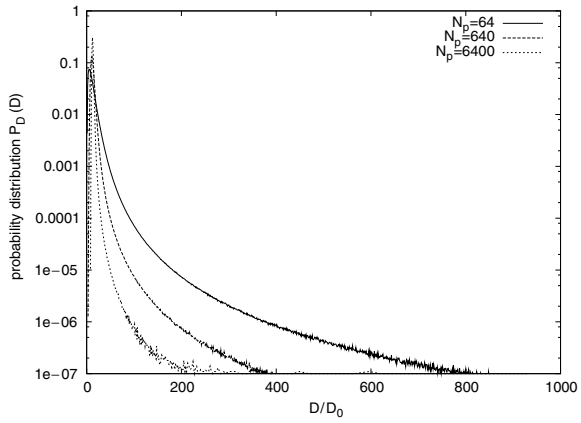

Figure B1. Probability density function $P_D(D)$ for D^{∞} from the result of the LIM. The function is computed by 10^9 realizations for $N_p = 64$ and $N_p = 640$, and for 10^8 realizations for $N_p = 6400$, $q_0 = 0.1$, and $\epsilon = 0.01$ ($D_0 = 0.01\mathrm{m}^2/\mathrm{day}$).

Figure B1 depicts the probability function for $t \to \infty$ and $N_p = 64, 640$ and $N_p = 6400$. Fitting the tail of the numerical results to a function proportional to $D^{-\alpha}$ using a nonlinear least-squares Marquardt–Levenberg algorithm [15] yields

$$\begin{aligned} \alpha &= 3.06 \pm 0.03 \qquad \text{for } N_p = 64 \qquad (D/D_0 \geqslant 600) \\ \alpha &= 3.01 \pm 0.02 \qquad \text{for } N_p = 640 \qquad (D/D_0 \geqslant 170) \\ \alpha &= 2.96 \pm 0.03 \qquad \text{for } N_p = 6400 \qquad (D/D_0 \geqslant 20). \end{aligned}$$

These numerical results agree with the analytical result (11) and show that the sample-to-sample fluctuations do not converge for $t \to \infty$. In particular, the asymptotic values of $P_D(D)$ are the smaller the larger N_p for fixed parameters q_0 and ϵ.

References

[1] Clincy M and Kinzelbach H 2001 Stratified disordered media: exact solutions for transport parameters and their self-averaging properties *J. Phys. A: Math. Gen.* **34** 7141–52

[2] Dagan G 1987 Theory of solute transport by groundwater *Water Resour. Res.* **19** 183–215

[3] Dagan G 1989 *Flow and Transport in Porous Formations* (Berlin: Springer)

[4] Dentz M, Kinzelbach H, Attinger S and Kinzelbach W 2000 Temporal behavior of a solute cloud in a heterogeneous porous medium: 1. Point-like injection *Water Resour. Res.* **36** 3591–604

[5] Dentz M, Kinzelbach H, Attinger S and Kinzelbach W 2002 Temporal behavior of a solute cloud in a heterogeneous porous medium: 3. Numerical simulations *Water Resour. Res.* **38** 23.1–23.13

[6] Dentz M, Kinzelbach H, Attinger S and Kinzelbach W 2003 Numerical studies of the transport behavior of a passive solute in a two-dimensional incompressible random flow field *Phys. Rev.* E **67** 1–10

[7] Eberhard J 2004 Approximations for transport parameters and self-averaging properties for point-like injections in heterogeneous media *J. Phys. A: Math. Gen* **37** 2549–71

[8] Gardiner C W 1985 *Handbook of Stochastic Methods (for Physics, Chemistry and Natural Science)* (New York: Springer)

[9] Gelhar L W 1993 *Stochastic Subsurface Hydrology* (Englewood Cliffs, NJ: Prentice Hall)

[10] Guyon E, Mitescu C D, Hulin J and Roux S 1989 Fractals and percolution in porous media and flows? *Physica* D **38** 172–8

[11] Jaekel U and Vereecken H 1997 Renormalization group analysis of macrodispersion in a directed random flow *Water Resour. Res.* **33** 2287–99

[12] Janković I, Fiori A and Dagan G 2003 Flow and transport in highly heterogeneous formations: 3. Numerical simulations and comparison with theoretical results *Water Resour. Res.* **39** 16.1–16.13
[13] Kesten H and Papanicolaou G C 1979 A limit theorem for turbulent diffusion *Commun. Math. Phys.* **65** 97–128
[14] Lenormand R and Zarcone C 1985 Invasion percolation in an etched network: measurement of a fractal dimension *Phys. Rev. Lett.* **54** 2226–9
[15] Press W H, Teukolsky S A, Vetterling W T and Flannery B P 1992 *Numerical Recipes in C: The Art of Scientific Computing* (Cambridge, UK: Cambridge University Press)
[16] Schwarze H, Jaekel U and Vereecken H 2001 Estimation of macrodispersion by different approximation methods for flow and transport in randomly heterogeneous media *Transp. Porous Media* **43** 265–87
[17] Suciu N, Vamoş C and Eberhard J 2006 Evaluation of the first-order approximations for transport in heterogeneous media *Water Resour. Res.* **42** W11504 (doi:10.1029/2005WR004714) pp 1–5
[18] Suciu N, Vamoş C, Vanderborght J, Hardelauf H and Vereecken H 2006 Numerical investigations on ergodicity of solute transport in heterogeneous aquifers *Water Resour. Res.* **42** W04409 (doi:10.1029/2005WR004546) pp 1–17
[19] Trefry M G, Ruan F P and McLaughlin D 2003 Numerical simulations of preasymptotic transport in heterogeneous porous media: departures from the Gaussian limit *Water Resour. Res.* **39** 10 1–12
[20] van Kampen N G 1981 *Stochastic Processes in Physics and Chemistry* (Amsterdam: North-Holland)
[21] Winter C L, Newman C M and Neuman S P 1984 A perturbation expansion for diffusion in random velocity field *SIAM J. Appl. Math.* **44** 411–24